

Aromaticity-Driven Rupture of CN Triple and CC Double Bonds: Mechanism of the Reaction between $\text{Cp}_2\text{Ti}(\text{C}_4\text{H}_4)$ and RCN

Cherumuttathu H. Suresh*[†] and Nobuaki Koga*[‡]

Computational Modeling and Simulation Section, Regional Research Laboratory (CSIR), Thiruvananthapuram 695 019, India, and Graduate School of Information Science, Nagoya University, Nagoya 464 8601, Japan

Received February 1, 2006

The mechanism of the unique reaction of $\text{Cp}_2\text{Ti}(\text{C}_4\text{H}_4)$ with MeCN yielding benzene and pyridine is unraveled using the DFT method. This reaction is characterized by the cleavage of two CC double bonds and one CN triple bond. Two separate mechanisms have been determined for these bond cleavages, wherein the first one involves two and the second one involves three MeCN molecules. In both these mechanisms, aromaticity-driven steps are identified on the basis of delocalized electronic structures, energetic stabilization, and significant NICS values of the intermediates. The aromaticity is a dominant factor for the high exothermicity of 65.8 kcal/mol found in the second mechanism. The third MeCN was very important for the CN triple bond breaking stage of the second mechanism, as it stabilized the titanium nitride intermediate by forming an aromatic TiNCN titanacycle. The π orbitals of the intermediate 4π -electron TiCCC and TiNCN titanacycles are found to be stabilized by participation of a vacant Ti “d” orbital in the 4π -electron conjugation, which is an important factor of aromaticity in metalloaromatic systems. Moreover, the agostic bonding interactions of the type recently identified in ruthenacyclobutanes have also been found in the intermediate 4π -electron titanacycles. Similar bonding interactions also occur in the 4π -electron tungstenacyclobutadiene of the Schrock complex $\text{W}[\text{CHCHCH}]\text{Cl}_3$. To our knowledge, this reaction is the first theoretical study of an aromaticity-driven organo-transition metal reaction.

Introduction

Many reactions in organo-transition metal chemistry are quite complicated and intriguing to explain in simple terms, and understanding the mechanism of such reactions still represents a major challenge for experimental as well as theoretical chemists. In fact, our knowledge on the reactive possibility of organo-transition complexes is far from complete, and many people believe that these complexes are the most important source of new reactions in organic synthesis. For instance, the transition metal-mediated cleavage of CX type bonds (X = H, first- and second-row main elements), particularly the CH and CC bonds, has been of great interest because of its applicability to organic synthesis.^{1–11} A number of noteworthy achievements, especially for the CC single bond cleavage, have been made in

the last two decades.^{11–21} However, only a few successful examples are known for the cleavage of CC double, CC triple, and CN triple bonds.^{21–30} Schrock’s metathesis reaction on a multiply bonded dinuclear tungsten complex is well-known for CC and CN triple bond cleavage.²² The Ritter reaction is a

* Corresponding authors. E-mail: sureshch@csrrtrd.ren.nic.in; koga@is.nagoya-u.ac.jp.

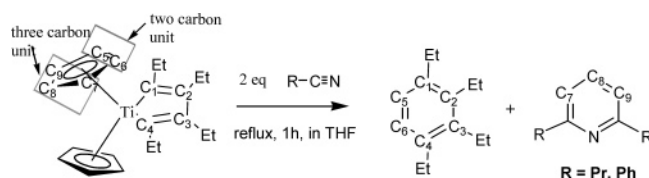
[†] Computational Modeling and Simulation Section, CSIR.

[‡] Nagoya University.

- (1) Murakami, M.; Ito, Y. *Activation of Unreactive Bonds and Organic Synthesis*; Springer: Berlin, 1999; pp 97–129.
- (2) Rybtchinski, B.; Milstein, D. *Angew. Chem., Int. Ed.* **1999**, *38*, 870.
- (3) Jennings, P. W.; Johnson, L. L. *Chem. Rev.* **1994**, *94*, 2241.
- (4) Jun, C. H.; Lee, J. H. *Pure Appl. Chem.* **2004**, *76*, 577–587.
- (5) Biswas, B.; Sugimoto, M.; Sakaki, S. *Organometallics* **2000**, *19*, 3895–3908.
- (6) Deckers, P. J. W.; Hessen, B. *Organometallics* **2002**, *21*, 5564–5575.
- (7) Jun, C. H. *Chem. Soc. Rev.* **2004**, *33*, 610–618.
- (8) Baker, R. T.; Calabrese, J. C.; Harlow, R. L.; Williams, I. D. *Organometallics* **1993**, *12*, 830–841.
- (9) Stephan, D. W.; Stewart, J. C.; Guerin, F.; Courtenay, S.; Kickham, J.; Hollink, E.; Beddie, C.; Hoskin, A.; Graham, T.; Wei, P. R.; Spence, R. E. V.; Xu, W.; Koch, L.; Gao, X. L.; Harrison, D. G. *Organometallics* **2003**, *22*, 1937–1947.
- (10) van der Heijden, H.; Hessen, B. *Inorg. Chim. Acta* **2003**, *345*, 27–36.

- (11) Hill, G. S.; Puddephatt, R. J. *Organometallics* **1998**, *17*, 1478–1486.
- (12) Crabtree, R. H.; Dion, R. P. *J. Chem. Soc., Chem. Commun.* **1984**, 1260.
- (13) Suggs, J. W.; Jun, C.-H. *J. Am. Chem. Soc.* **1986**, *108*, 4679.
- (14) Bunel, E.; Burger, B. J.; Bercaw, J. E. *J. Am. Chem. Soc.* **1988**, *110*, 976.
- (15) Hartwig, J. F.; Andersen, R. A.; Bergman, R. G. *J. Am. Chem. Soc.* **1989**, *111*, 2717.
- (16) Gozin, M.; Weisman, A.; Ben-David, Y.; Milstein, D. *Nature* **1993**, *364*, 699.
- (17) Suginome, M.; Matsuda, T.; Ito, Y. *J. Am. Chem. Soc.* **2000**, *122*, 11015.
- (18) Nishimura, T.; Araki, H.; Maeda, Y.; Uemura, S. *Org. Lett.* **2003**, *5*, 2997.
- (19) Lee, D. Y.; Kim, I. J.; Jun, C. H. *Angew. Chem., Int. Ed.* **2002**, *41*, 3031–3033.
- (20) Miller, J. A. *Tetrahedron Lett.* **2001**, *42*, 6991–6993.
- (21) Rybtchinski, B.; Vigalok, A.; BenDavid, Y.; Milstein, D. *J. Am. Chem. Soc.* **1996**, *118*, 12406–12415.
- (22) Schrock, R. R.; Listemann, M. L.; Sturgeooff, L. G. *J. Am. Chem. Soc.* **1982**, *104*, 4291–4293.
- (23) Moriarty, R. M.; Penmasta, R.; Awasthi, A. K.; Prakash, I. *J. Org. Chem.* **1988**, *53*, 6124.
- (24) Sawaki, Y.; Inoue, H.; Ogata, Y. *Bull. Chem. Soc. Jpn.* **1983**, *56*, 1133.
- (25) Früstner, A.; Mathes, C.; Lehmann, C. W. *Chem. Eur. J.* **2001**, *7*, 5299.
- (26) Ananikov, V. P.; Musaev, D. G.; Morokuma, K. *Organometallics* **2001**, *20*, 1652–1667.
- (27) Lim, S. G.; Jun, C. H. *Bull. Korean Chem. Soc.* **2004**, *25*, 1623–1624.
- (28) de Jesus, J. C.; Zaera, F. *J. Mol. Catal. A-Chem.* **1999**, *138*, 237–240.

Scheme 1



famous reaction know to activate CN triple bonds.³¹ Recently, Rybak-Akimova et al. have observed strong CN triple bond activation in a condensation reaction when acetonitrile reacted with a dinuclear nickel(II) complex.³² The iridium hydride catalyst $IrH(CO)(PPh_3)_3$ discovered by Murahashi and co-workers is found to be very effective for the complete activation of CN triple bond in nitriles.³³

In the present work we are interested in the reaction of a biscyclopentadienyl-titanacyclobutadiene complex recently reported by Takahashi et al.,³⁴ which is given in Scheme 1. One of the products of the reaction was a substituted benzene, and its arene ring contained two adjacent carbon atoms derived from one of the Ti-bound Cp ligands, whereas the second product pyridine contained the three remaining carbon atoms of this ligand. This reaction was sure to involve the rupture of CC and CN multiple bonds. Although the CC multiple bond cleavage was quite evident in the experimental results, attention was not paid to the obvious aspect of the CN triple bond cleavage.³⁴ In fact, proposing a mechanism for the CN bond activation is very challenging from intuitive chemical knowledge alone. Therefore, we decided to undertake a theoretical study of this reaction, as it can truly enhance our understanding and appreciation of the reactive possibilities of transition metals. Hence, a quantum chemical modeling is performed to get a plausible and complete mechanism of this unique reaction. In the present work, using the density functional theory (DFT) method and model molecules $Cp_2Ti(C_4H_4)$ (**1**) and MeCN, we explored such a mechanism.

Computational Methods

All the molecular geometries were optimized at the DFT level by using Becke's three-parameter exchange functional (B3)^{35,36} in conjunction with the Lee–Yang–Parr correlation functional (LYP)³⁷ as implemented in the Gaussian 03 suite of programs.³⁸ For Ti, the basis set LanL2DZ was used.^{39–41} For H, C, and N, 6-31G(d) basis functions were selected.⁴² The DFT method thus employed is denoted as B3LYP/Gen1. Normal coordinate analysis has been performed for all stationary points to characterize the transition states and minimum structures. Therefore, the energy minimum structures reported in this paper show positive eigenvalues of the Hessian matrix, whereas transition states (TSs) have one negative eigenvalue. For most TSs, the analysis including the visualization

(29) Datka, J.; Broclawik, E.; Kozyra, P.; Kukulka-Zajac, E.; Bartula, D.; Szutiak, M. The activation of C=C bond in alkenes by Cu^+ ions in zeolites IR, TPD-IR studies and DFT calculations. In *Recent Advances In The Science and Technology of Zeolites and Related Materials, Pts A–C*; Elsevier: Amsterdam, 2004; Vol. 154, pp 2151–2156.

(30) Chisholm, M. H. *Chem. Rec.* **2001**, *1*, 12–23.

(31) Reddy, K. L. *Tetrahedron Lett.* **2003**, *44*, 1453–1455.

(32) Kryatov, S. V.; Nazarenko, A. Y.; Smitha, M. B.; Rybak-Akimova, E. V. *Chem. Commun.* **2001**, 1174–1175.

(33) Takaya, H.; Naota, T.; Murahashi, S.-I. *J. Am. Chem. Soc.* **1998**, *120*, 4244–4245.

(34) Xi, Z.; Sato, K.; Gao, Y.; Lu, J.; Takahashi, T. *J. Am. Chem. Soc.* **2003**, *125*, 9568.

(35) Becke, A. D. *J. Chem. Phys.* **1993**, *98*, 5648.

(36) Becke, A. D. *J. Chem. Phys.* **1993**, *98*, 5648–5652.

(37) Lee, C. T.; Yang, W. T.; Parr, R. G. *Phys. Rev. B* **1988**, *37*, 785–789.

of the negative frequency was sufficient to specify the corresponding reaction path. In some cases, intrinsic reaction coordinate (IRC) calculations^{43,44} near the TS region followed by geometry optimization of both reactants and products were performed to confirm the connectivity of the TSs. Unscaled vibrational frequencies were used to calculate zero-point energy (ZPE) correction to the total energy. The Gibbs free energies were also calculated employing the usual approximations of statistical thermodynamics (ideal gas, harmonic oscillator, and rigid rotor) at a temperature of 298.15 K and a pressure of 1.00 atm. Unless otherwise noted, the Gibbs free energy changes are used throughout in the text.

Using the B3LYP/Gen1 level optimized geometry, absolute NMR shielding values were calculated for selected systems by the gauge-independent atomic orbital (GIAO) method⁴⁵ at the B3LYP/6-311++G** level of theory. Further, nucleus-independent chemical shift (NICS) values were obtained by calculating absolute NMR shielding at ring centers. NICS values pioneered by Schleyer were used as a descriptor of aromaticity from the magnetic point of view. A negative NICS value denotes aromaticity. For instance, a NICS value of around -10.0 ppm is observed in the case of benzene (this value varies slightly depending on the method and basis set employed). A positive value of NICS shows antiaromaticity, while small NICS values close to zero indicate nonaromaticity.

Results and Discussion

A. Geometry of Titanocene Metallacycle 1. In Figure 1, the optimized geometry of titanacyclopentadiene system **1** is depicted along with the TSs and intermediates for the formation of benzene. The Cp ligands in **1** are in staggered arrangement, and its Ti–C₄, C₄–C₃, and C₃–C₂ distances are 2.119, 1.354, and 1.465 Å, respectively. Further, the Cp carbon atoms C₅ and C₆ are at the same distance of 2.807 Å from C₁ and C₄, respectively, of the butadiene-1,4-diyl moiety. This distance is well within the sum of van der Waals radii⁴⁶ of two carbon atoms, and therefore a small twist or turn in the Cp ligand or the butadiene-1,4-diyl moiety can lead to the closer approach of the Cp carbon atoms to the butadiene-1,4-diyl moiety, resulting in a migration or an insertion reaction between them. We explore this possibility by doing a transition state search for the C₁–C₅ bond formation.

B. Migratory Insertion of the Carbon Atoms of the Cp Ligand. The transition state **TS1** is located for the C₁–C₅ bond formation. Compared to **1**, in this TS the bond from the C_α carbon C₁ to Ti (Ti–C₁) is almost broken and strong bonding

(38) Frisch, M. J.; Trucks, G. W.; Schlegel, H. B.; Scuseria, G. E.; Robb, M. A.; Cheeseman, J. R.; Montgomery, J., J. A.; Vreven, T.; Kudin, K. N.; Burant, J. C.; Millam, J. M.; Jeng, S. S.; Tomasi, J.; Barone, V.; Mennucci, B.; Cossi, M.; Scalmani, G.; Rega, N.; Petersson, G. A.; Nakatsuji, H.; Hada, M.; Ehara, M.; Toyota, K.; Fukuda, R.; Hasegawa, J.; Ishida, M.; Nakajima, T.; Honda, Y.; Kitao, O.; Nakai, H.; Klene, M.; Li, X.; Knox, J. E.; Hratchian, H. P.; Cross, J. B.; Bakken, V.; Adamo, C.; Jaramillo, J.; Gomperts, R.; Stratmann, R. E.; Yazyev, O.; Austin, A. J.; Cammi, R.; Pomelli, C.; Ochterski, J. W.; Ayala, P. Y.; Morokuma, K.; Voth, G. A.; Salvador, P.; Dannenberg, J. J.; Zakrzewski, V. G.; Dapprich, S.; Daniels, A. D.; Strain, M. C.; Farkas, O.; Malick, D. K.; Rabuck, A. D.; Raghavachari, K.; Foresman, J. B.; Ortiz, J. V.; Cui, Q.; Baboul, A. G.; Clifford, S.; Cioslowski, J.; Stefanov, B. B.; Liu, G.; Liashenko, A.; Piskorz, P.; Komaromi, I.; Martin, R. L.; Fox, D. J.; Keith, T.; Al-Laham, M. A.; Peng, C. Y.; Nanayakkara, A.; Challacombe, M.; Gill, P. M. W.; Johnson, B.; Chen, W.; Wong, M. W.; Gonzalez, C.; Pople, J. A. *Gaussian 03, Revision C.02*; Gaussian, Inc.: Wallingford, CT, 2004.

(39) Hay, P. J.; Wadt, W. R. *J. Chem. Phys.* **1985**, *82*, 299–310.

(40) Hay, P. J.; Wadt, W. R. *J. Chem. Phys.* **1985**, *82*, 270–283.

(41) Wadt, W. R.; Hay, P. J. *J. Chem. Phys.* **1985**, *82*, 284–298.

(42) Hariharan, P. C.; Pople, J. A. *Mol. Phys.* **1974**, *27*, 209.

(43) Fukui, K. *Acc. Chem. Res.* **1981**, *14*, 363.

(44) González, C.; Schlegel, H. B. *J. Chem. Phys.* **1991**, *95*, 5853.

(45) Ditchfield, R. *Mol. Phys.* **1974**, *27*, 789.

(46) Bondi, A. *J. Phys. Chem.* **1964**, *68*, 441–451.

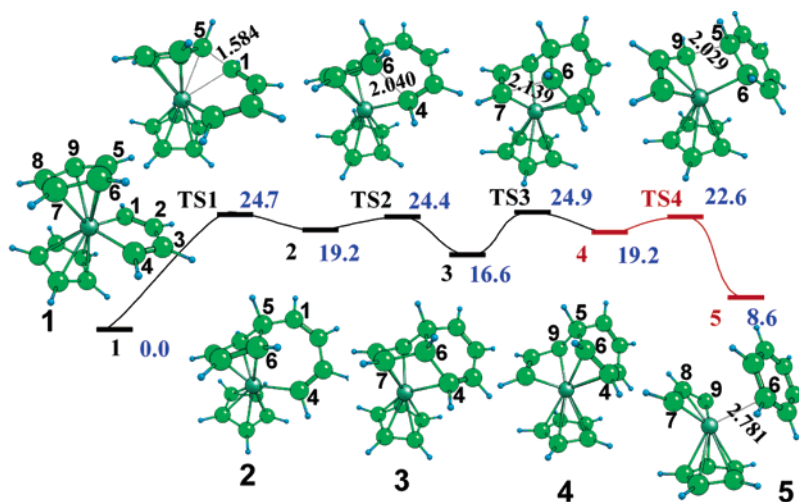


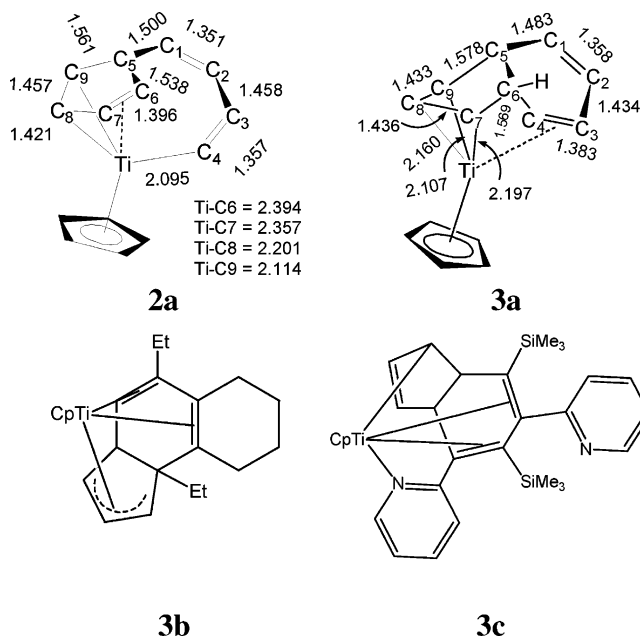
Figure 1. Migratory insertion of C₅ into the Ti–C₁ bond of **1** and subsequent cleavage of the Cp ring CC bonds. Aromaticity-driven step is shown in red. Relative free energy is in kcal/mol (blue) and distances are in angstroms. Atom numbering is also shown.

interaction takes place between the Cp carbon C₅ and C₁ at a distance of 1.584 Å. The resulting intermediate product from **TS1** is **2**. In **2**, the C₆–C₇ bond distance 1.396 Å is considered as a double bond having η² coordination with Ti. This weak π coordination gives long bond lengths of 2.394 and 2.357 Å for Ti–C₆ and Ti–C₇ bonds, respectively. On the other hand, the bond length values of 2.201, 2.114, and 1.457 Å observed for Ti–C₈, Ti–C₉, and C₈–C₉, respectively, are indicative of their σ bond character. The schematic structure **2a** is suitable for **2**, and on that basis, the transformation of **1** to **2** is considered as a migratory insertion process of the Cp carbon atom into the Ti–C bond. The free energy of activation for this step is found to be 24.7 kcal/mol. It may be noted that the C₁–C₅ bond formation in **2** destroys its aromatic Cp ligand as well as the aromatic titanacyclobutadiene ring, and the compound itself is now a 14-electron system. We believe that the 14-electron configuration as well as the loss of a substantial amount of aromaticity in **2** is the main reason for the high endothermicity of 19.2 kcal/mol observed for the **1** to **2** conversion.

In complex **2**, the α-carbon C₄ is only 2.678 Å from the nearest Cp carbon, and as a result, **2** quickly passes through **TS2** with an activation energy of 5.2 kcal/mol. The visualization of the imaginary frequency of **TS2** suggested the bonding interaction between C₄ and C₆ at a distance of 2.040 Å. The product **3** formed from **TS2** has a relative energy of 16.6 kcal/mol. The two-carbon unit composed of C₅ and C₆ of the Cp ring in **3** is mostly freed from any significant interaction with the metal atom. Also in **3**, if the carbon atoms of the C₇C₈C₉ unit are connected via σ bonds to Ti and C₄–C₃ (1.383 Å) is π-coordinated to Ti, the oxidation state of the metal will be +4 and the schematic structure **3a** can be drawn for it. On the other hand, if we consider that the Ti is bound to an allylic three-carbon unit (C₇C₈C₉), the formal electron count would give a +2 oxidation state for Ti. A molecular orbital analysis of **3** showed no occupied “d” orbital, and that supported a +4 oxidation state for the metal. Therefore, the conversion of **2** to **3** is considered as a CC bond coupling reaction. In **3**, the C₅–C₆ unit originally coming from the Cp ligand becomes a part of a six-membered ring. This six-membered ring composed of the C₁C₂C₃C₄C₅C₆ region can be visualized as a precursor structure for benzene formation.

Experimental support is also available for the intramolecular rearrangement described in the above two paragraphs. For instance, a reaction similar to the **1** to **2** conversion was already discovered two decades ago by Rosenthal et al.,^{43,47} who

conducted reactions at ambient temperature with the bicyclic titanacyclobutadiene derivative of **1** as well as with the complex Cp₂TiC(SiMe₃)=C(Py)C(SiMe₃)=C(Py) and obtained the X-ray structure of **3b** and **3c**. Structure **3b** is very similar to **3a**, except that in **3b** both the double bonds in the six-membered ring are π-coordinated to the metal atom. It may be seen that a simple structural rearrangement in **3a** would lead to the formation of a structure with the same metal–ligand bonding as that in **3b**. Complex **3c** is also formed as a result of intramolecular CC bond coupling followed by the intramolecular coordination of the α-pyridyl substituent to the metal atom.



C. Rupture of CC Bonds Leading to the Formation of Benzene

In the next two consecutive steps, viz., **3** → **TS3** → **4** and **4** → **TS4** → **5**, the unprecedented double CC bond cleavage (C₆–C₇ and C₅–C₉) of the Cp ring observed in the experiment of Takahashi et al.³⁴ is unraveled (Figure 1). The *E*_{act} of the former and the latter steps are 8.3 and 3.4 kcal/mol, respectively. An allylic moiety composed of a C₃C₄C₆ unit is

(47) Rosenthal, U.; Lefebvre, C.; Arndt, P.; Tillack, A.; Baumann, W.; Kempe, R.; Burlakov, V. V. *J. Organomet. Chem.* **1995**, *503*, 221.

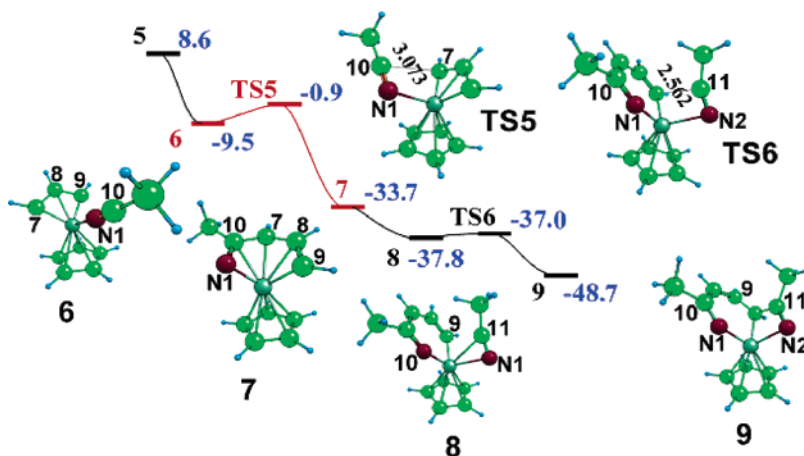
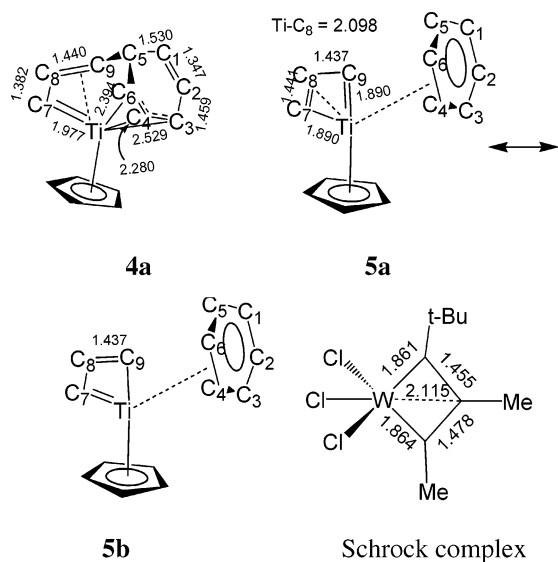


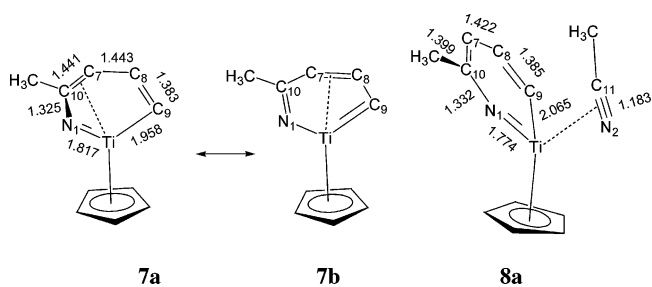
Figure 2. Activation of CN triple bonds in MeCN. Aromaticity-driven step is shown in red. Relative free energy is in kcal/mol (blue) and distances are in angstroms. Atom numbering is also shown.

identified in structure **4**. Its Ti–C₇ bond of length of 1.977 Å has significant double-bond character, and the C₈–C₉ bond is only 2.394 Å away from the metal. Therefore, the schematic structure **4a** is suggested for **4**, which means that Ti is in the +4 oxidation state. Therefore, the **3** to **4** conversion is considered as a simple CC bond cleavage reaction.



The low activation barrier and the high exothermicity of 10.6 kcal/mol of the step **4** → **TS4** → **5** can be explained when we invoke aromaticity. Since the aromatization energy of benzene is around 30.0 kcal/mol,^{48,49} we can assume that the formation of loosely Ti-bound benzene complex **5** brings that much aromatic stabilization energy to the system and that also accounts for the exothermicity of the reaction. Even the four-membered titanacycle^{50,51} defined by TiC₇C₈C₉ of **5** attains some stabilizing π -delocalization effect because the bond lengths of 1.890, 1.890, 1.441, and 1.437 Å observed for Ti–C₇, Ti–C₉, C₇–C₈, and C₈–C₉, respectively, suggest that **5** can be represented by a resonance combination of the structures **5a** and **5b**. The Ti–C₈ distance of 2.098 Å is quite short in this complex and is even shorter than the Ti–C _{α} single bond length in **1**. It may be

noted that any experimental evidence to support the existence of the 12-electron species CpTi[CHCHCH] found in **5** would further strengthen the validity of the present mechanism. This complex may be difficult to detect because the 12-electron Ti would be highly reactive. Instead of a 12-electron Ti species such as CpTi[CHCHCH], examples exist of heavier group metals especially of group 6 metals. For instance the X-ray structure of the complex W[C(t-Bu)CMeCMe]Cl₃ was reported by Schrock et al. more than two decades ago.⁵² Like in the case of **5**, this tungsten complex too showed a short W–C _{β} bond of length 2.115 Å (see the schematic structure of W[C(t-Bu)CMeCMe]Cl₃, showing the bond length parameters obtained from the X-ray geometry).



D. Coordination of the First and Second CH₃CN to Ti and Activation of CN Triple Bonds. An incoming MeCN molecule can easily displace the loosely bound benzene in **5**. This step giving **6** is exothermic by 18.1 kcal/mol (Figure 2). A slight amount of slippage of MeCN from its end-on coordination in **6** leads to the early transition state **TS5** (E_{act} = 8.6 kcal/mol), which shows a weak bonding interaction between C₇ and MeCN carbon C₁₀ at a distance of 3.073 Å. From **TS5**, the product of MeCN insertion into the Ti–C₇ bond forms **7** is a quite stable metallaheterocycle, which is placed at a relative energy of –33.9 kcal/mol as compared to complex **1**. In **7**, the bond lengths of Ti–C₉, Ti–N₁, N₁–C₁₀, C₁₀–C₇, C₇–C₈, and C₈–C₉ are 1.958, 1.817, 1.325, 1.441, 1.443, and 1.383 Å, respectively, suggesting significant double-bond character for all of them. Therefore, a resonance combination of two structures, **7a** and **7b**, is assigned for it. The higher stability of complex **7** is thus accounted for by the delocalized nature of

(48) Schleyer, P. v. R.; Puhlhofer, F. *Org. Lett.* **2002**, *4*, 2873.

(49) Suresh, C. H.; Koga, N. *J. Org. Chem.* **2002**, *67*, 1965.

(50) Lugo, A.; Fischer, J.; Lawson, D. B. *J. Mol. Struct. (THEOCHEM)* **2004**, *674*, 139.

(51) Iron, M. A.; Martin, J. M. L.; van der Boom, M. E. *J. Am. Chem. Soc.* **2003**, *125*, 13020.

(52) Pedersen, S. F.; Schrock, R. R.; Churchill, M. R.; Wasserman, H. *J. Am. Chem. Soc.* **1982**, *104*, 6808–6809.

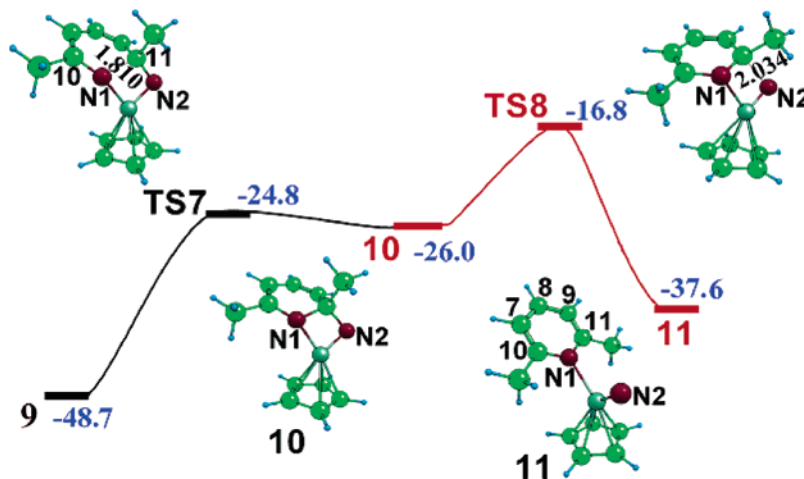


Figure 3. Rupture of CN triple bond via the reaction of two MeCN molecules to titanium. Aromaticity-driven step is shown in red. Relative free energy is in kcal/mol (blue) and distances are in angstroms. Atom numbering is also shown.

the six π electrons in the metallaheterocycle,^{50,51} which means significant aromatic character for **7**. Thus, **6** to **7** conversion (Figure 2) is also considered an aromaticity-driven process. The highlight of this part of the reaction is the substantial activation of the CN triple bond by consuming only 8.4 kcal/mol in energy.

At this stage, a second MeCN molecule coordinates to **7** via its CN π electrons (Figure 2). The complex **8** thus formed is further stabilized by 4.0 kcal/mol. Interestingly, unlike **7**, the metallaheterocycle unit $\text{TiN}_1\text{C}_{10}\text{C}_7\text{C}_8\text{C}_9$ is planar, and it shows a lesser degree of delocalized nature of the six π electrons (see schematic structure **8a**). From **8**, nearly a barrierless process for the insertion of the Ti–C₉ bond to Ti–C₁₁ occurs. The resulting product **9** is quite stable at the relative energy of –48.7 kcal/mol. The C₁₁–N₂ triple bond (1.183 Å) in complex **8** is clearly activated to a C₁₁–N₂ double bond (1.281 Å) in complex **9** with almost no cost in energy.

E. Rupture of CN Triple Bonds. We have considered two possibilities for the further activation of C₁₁–N₂ double bond in **9**. In the first possibility, the CN activation is observed when **9** passes through **TS7** leading to the formation of **10**. Intermediate **10** contains the precursor heterocyclic moiety for the pyridine formation, which is depicted in Figure 3. However, this step needs a relatively high E_{act} of 23.9 kcal/mol. The C₁₁–N₂ bond breaks away from complex **10** when it passes through **TS8**, which gives rise to the pyridine-bound titanium nitride **11**. The E_{act} for this step of the reaction is only 9.2 kcal/mol, and it is exothermic by 11.6 kcal/mol. The overall activation energy for the combined steps of **9** → **TS7** → **10** → **TS8** → **11** has gone up to 31.9 kcal/mol, and the reaction is also endothermic by 11.1 kcal/mol. In terms of the energetics, this is not very favorable for the reaction. Although, **11** has more energy than **9**, the formation of this complex in the mechanism is interesting because, in the experiment, Takahashi et al. have reported the formation of NH_3 , and a reasonable reaction for its generation is thought to be the hydrolysis of a titanium nitride complex. Such a hydrolysis reaction may require complicated multistep hydrogen transfer processes, and because the focus of this work is on the formation of benzene and pyridine, further reaction of **11** with water was not attempted.

For the second possibility, the reaction of a third MeCN to the most stable intermediate **9** is considered. Such a reaction gives **13** through the metastable intermediate **12** and **TS9** (Figure 4). The E_{act} is found to be 21.2 kcal/mol. From **13**, the formation of the six-membered heterocycle system **14** is very easy (see **TS10**; E_{act} = 3.6 kcal/mol). The next step (**14** → **TS11** → **15**)

gives pyridine, which is an aromaticity-driven process, as it shows low activation energy (E_{act} = 10.0 kcal/mol) and a high exothermicity of 28.7 kcal/mol. In this step, the original C₁₁–N₂ triple bond of the second MeCN is completely cleaved. Thus, it is clear that the mechanism involving the third MeCN is the preferred one. A comparison of the structure and energies of **11** and **15** suggests that the third MeCN stabilizes the Ti–N triple bond by 28.2 kcal/mol.

F. Orbital Interactions in the Four-Membered Titanacycle Intermediates and the Related Schrock Complex $\text{W}[\text{CH}=\text{CHCH}]\text{Cl}_3$. The four-membered titanacycles TiCHCHCH in **5** and $\text{TiNC}(\text{CH}_3)\text{N}$ in **15** are structurally and electronically very interesting, structurally interesting because they show bond length equalization as well as a very short distance between Ti and the diagonally opposite carbon atom in the titanacycle. This Ti–C distance is found to be 2.098 Å in **5** and 2.072 Å in **15**, and these values are shorter than the single Ti–C _{α} bond lengths of 2.120 Å observed in the parent complex **1**. Electronically these titanacycles are like the 4 π electron Hückel systems, and such organic systems are usually antiaromatic. To understand the bonding in these systems, we have calculated the structure of systems CpTiCHCHCH (**16**) and $\text{CpTiNC}(\text{CH}_3)\text{N}$ (**17**) and analyzed their MOs. The optimized structure and the important MOs are presented in Figure 5.

The two occupied π orbitals MO29 and MO34 for **16** and MO32 and MO36 for **17** describe their π -bonding interactions. These π orbitals are stabilized by participation of vacant Ti “d” orbital in the conjugation, which is an important factor of aromaticity in metallaaromatic systems.^{53,54} The MO26 and MO33 in **16** and MO34 and MO37 in **17** are responsible for the bonding interaction between the metal atom and the carbon atom diagonally opposite it. This type of bonding interaction is observed in the case of the ruthenacyclobutane intermediate found in Grubb’s olefin metathesis reaction mechanism, and such a bonding is designated as agostic because the metal “d” orbital is in direct interaction with the CC σ bond in **16** or the CN σ bond in **17**.^{55,56} The agostic bond in **16** is α,β -(CCC) agostic, and that in **17** is α,β -(NCN) agostic. In the case of the

(53) Masui, H. *Coord. Chem. Rev.* **2001**, 219–221, 957–992.

(54) Huang, Y.-Z.; Yang, S.-Y.; Li, X.-Y. *J. Organomet. Chem.* **2004**, 689, 1050–1056.

(55) Suresh, C. H.; Koga, N. *Organometallics* **2004**, 23, 76–80.

(56) Suresh, C. H.; Baik, M.-H. *Dalton Trans.* **2005**, 2982–2984.

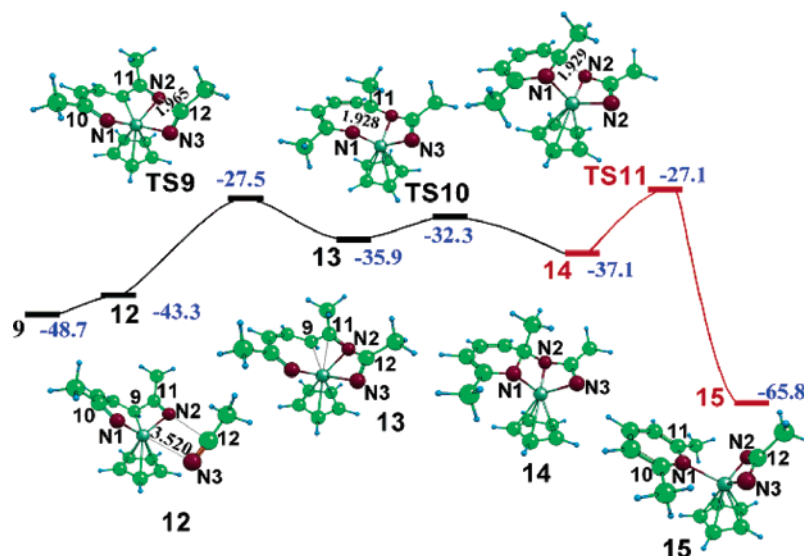


Figure 4. Rupture of CN triple bond via the reaction of three MeCN molecules to titanium. Aromaticity-driven step is shown in red. Relative free energy is in kcal/mol (blue) and distances are in angstroms. Atom numbering is also shown.

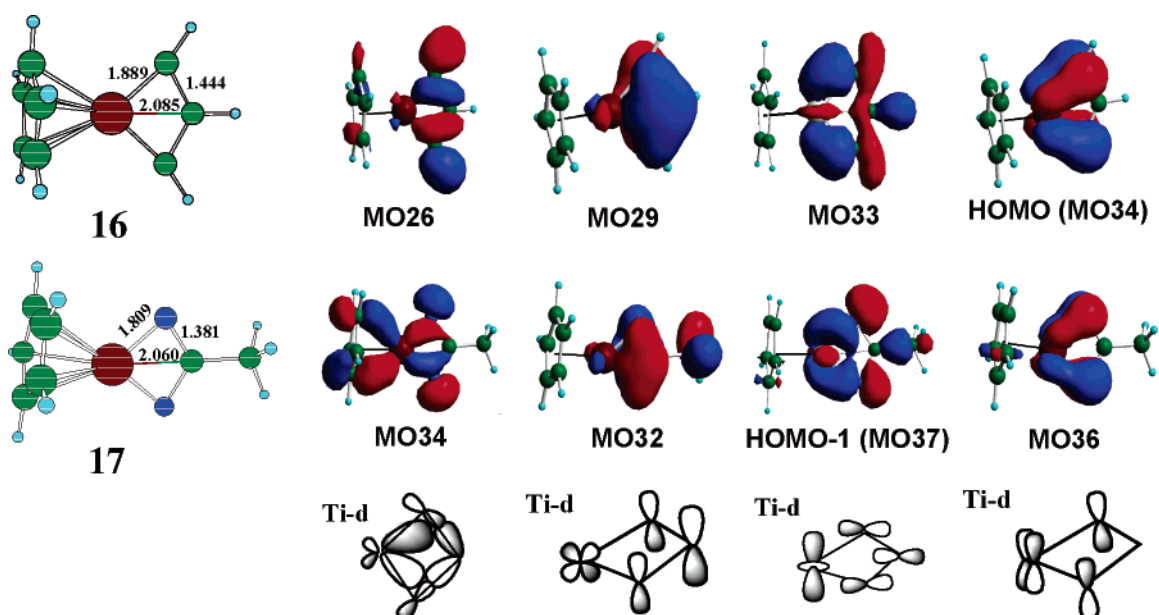


Figure 5. Molecular orbitals of titanacycle systems **16** and **17** showing the π bond and agostic interactions. See text for details. All bond lengths are in angstroms.

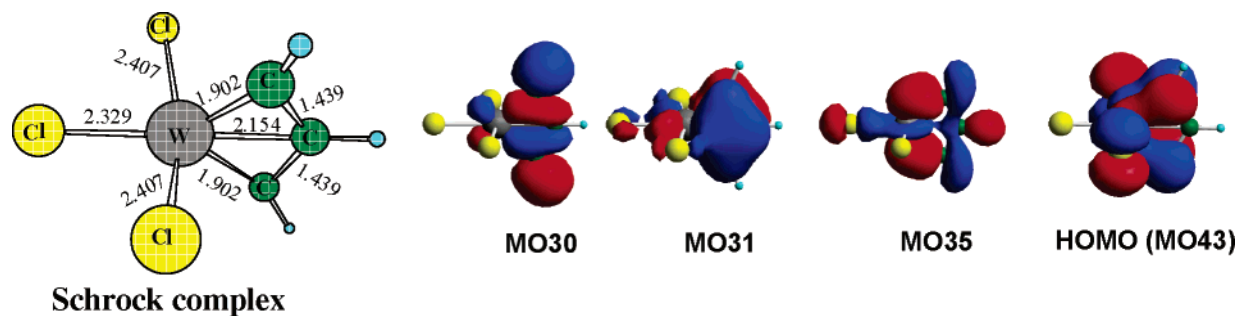


Figure 6. Molecular orbitals of Schrock complex showing the π bond and agostic interactions. All bond lengths are in angstroms.

Schrock complex $W[C(t-Bu)CMeCMe]Cl_3$ already mentioned in Section C, we may expect the same MO features for the metallacycle.⁵² To verify this, the unsubstituted metallacycle $W[CHCHCH]Cl_3$ was optimized at the B3LYP/Gen1 level and the MOs were analyzed (cf. Figure 6). The W–C and W–Cl distances of the optimized geometry were in good agreement

with the X-ray structure of $W[C(t-Bu)CMeCMe]Cl_3$. The MOs similar to those found in **16** and **17** were also detected in the tungstanacyclobutadiene complex.

G. NICS Analysis and Aromaticity. The phenomenon of aromaticity is one of the most widely used concepts in chemistry, particularly in organic chemistry.^{57,58} A compound is identified

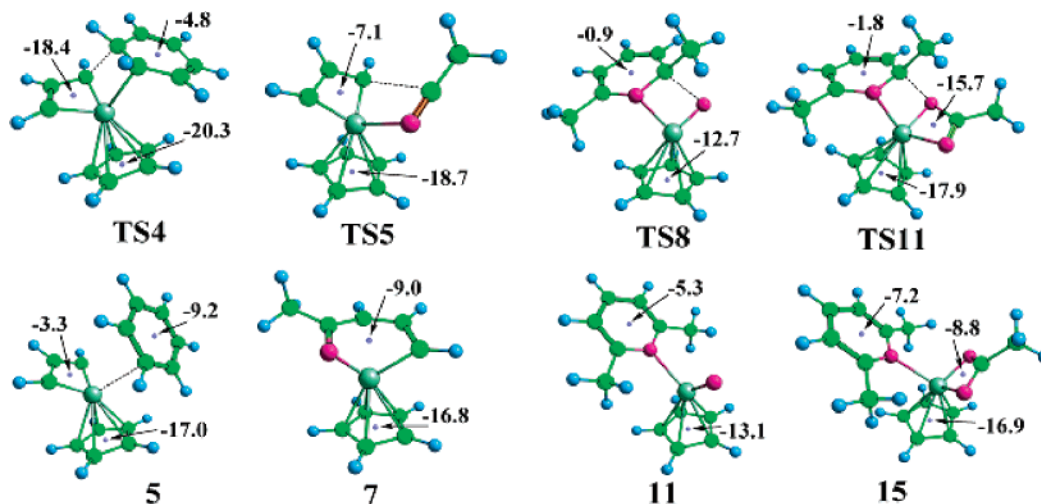


Figure 7. NICS values in ppm unit at the ring center of **TS4**, **TS5**, **TS8**, and **TS11** and their corresponding products **5**, **7**, **11**, and **15**.

as aromatic based on physicochemical evidence such as bond length equalization, planar structure, magnetic susceptibility increase, magnetic anisotropy, ring current, remarkable stability, and characteristic reactions of the systems. The study of aromaticity has become somewhat simplified after Schleyer et al.^{59–65} introduced NICS as an efficient magnetic criterion of aromaticity. On the basis of this criterion, it was even possible to understand aromaticity of transition states. For instance, it has been used as an effective probe of aromaticity in transition states of pericyclic reactions.^{60,61,66–68} So far the transition states of an organometallic reaction was not considered for NICS evaluation of aromaticity. Further, to our knowledge there is no theoretical study in the literature on the mechanism of an organo-transition metal reaction that focuses on the aromaticity factor. Therefore, in the present study, since we propose four aromaticity-driven processes, viz., (i) **4** → **TS4** → **5**; (ii) **6** → **TS5** → **7**; (iii) **10** → **TS8** → **11**; and (iv) **14** → **TS11** → **15**, it is felt that an NICS analysis is worth doing.

In Figure 7, the NICS values at the ring centers of the transition states **TS4**, **TS5**, **TS8**, and **TS11** and their corresponding products are depicted. The NICS value of -4.8 ppm in the six-membered ring of **TS4** clearly suggests its partial aromatization. In **5**, the benzene ring NICS value of -9.2 ppm indicates its full aromatization. Interestingly, the titanacyclobutadiene units in **TS4**, **5**, and **TS5** also show aromatic character. The high negative NICS value of the titanacyclobutadiene unit in **TS4** is due to its increased nonplanar structure (TiCCC twist is 13.6°) as compared to **5** (TiCCC twist is 1.4°) and **TS5**

(TiCCC twist is 2.3°). Such high negative NICS values were also observed in the nonplanar pericyclic transition state, and according to Schleyer et al.,⁶¹ that was due to the large in-plane σ orbital contribution. Aromatization of the six-membered N-heterocyclic metallacene unit in **7** is also observed (NICS = -9.0 ppm). However, the NICS value of -0.9 ppm observed for the N-heterocyclic unit in transition state **TS8** suggests only a small aromatic stabilization. As expected, once the **TS8** is converted to the product **11**, the aromatization of the pyridine ring occurs (NICS = -5.3 ppm). We can also see a substantial reduction in the aromatic character of the Cp anion ligand in **TS8** and **11** as compared to that of the other systems shown in Figure 5. In **TS11**, the six-membered heterocycle is weakly aromatic (NICS = -1.8 ppm), while its TiNCN titanacycle is highly aromatic (-15.7 ppm). The pyridine unit of **15** is more aromatic than that of **11**, and its TiNCN metallacycle retains a high amount of aromaticity (-8.8 ppm). The NICS-based assessment as well as the energetics are more supportive toward the three-acetonitrile-mediated reaction giving rise to **TS11** and **15** than the two-acetonitrile-mediated reaction consisting of **TS8** and **11**. Thus the NICS criterion as well as the energetics of the reaction supports the reaction steps **4** → **TS4** → **5**, **6** → **TS5** → **7**, and **14** → **TS11** → **15** as aromaticity-driven processes.

Conclusions

The energetics of the purely intramolecular part of the mechanism (**1** → **5**) as depicted in Figure 1 suggests that this mechanism is quite reasonable for the formation of benzene. In this mechanism, the intermediate structures **2**, **3**, and **4** formed before **5** are at high energy levels as compared to **1**. Further, once the first step of the reaction leading to the formation of **2**, the highest activation energy step in the whole reaction, is passed, the reaction steps from **2**, **3**, and **4** are relatively very easy because of their low activation barriers. Therefore, the possibility of an intermolecular mechanism in which the acetonitrile coordinates with the intermediates **2**, **3**, and **4** before the formation of **5** is less likely. The energetics and the NICS-based analysis suggests that compared to the two-MeCN-mediated mechanism (Figure 3), the three-MeCN-mediated mechanism (Figure 4) is more attractive for the CN triple bond breaking leading to the formation of pyridine. Based on the three-MeCN-mediated mechanism, the reaction between titanacyclopentadienyl complex **1** and acetonitrile giving rise to benzene and pyridine can be considered as a highly exothermic process. The aromaticity is a dominant factor for the high

(57) Schleyer, P. v. R. *Chem. Rev.* **2001**, *101*, 1115–1117.

(58) Minkin, V. J.; Glukhovtsev, M. N.; Simkin, B. Y. *Aromaticity and Antiaromaticity; Electronic and Structural Aspects*; Wiley: New York, 1994.
(59) Krygowski, T. M.; Ejsmont, K.; Stepień, B. T.; Cyrański, M. K.; Poater, J.; Solá, M. *J. Org. Chem.* **2004**, *69*, 6634.

(60) Jiao, H. J.; Nagelkerke, R.; Kurtz, H. A.; Williams, R. V.; Borden, W. T.; Schleyer, P. v. R. *J. Am. Chem. Soc.* **1997**, *119*, 5921–5929.

(61) Jiao, H. J.; Schleyer, P. v. R. *J. Phys. Org. Chem.* **1998**, *11*, 655–662.

(62) Jiao, H. J.; Schleyer, P. v. R.; Beno, B. R.; Houk, K. N.; Warmuth, R. *Angew. Chem., Int. Ed. Engl.* **1997**, *36*, 2761–2764.

(63) Erhardt, S.; Frenking, G.; Chen, Z. F.; Schleyer, P. v. R. *Angew. Chem., Int. Ed.* **2005**, *44*, 1078–1082.

(64) Lein, M.; Frunzke, J.; Frenking, G. *Angew. Chem., Int. Ed.* **2003**, *42*, 1303–1306.

(65) Schleyer, P. v. R.; Manoharan, M.; Wang, Z. X.; Kiran, B.; Jiao, H. J.; Puchta, R.; Hommes, N. *Org. Lett.* **2001**, *3*, 2465–2468.

(66) Zora, M. *J. Org. Chem.* **2004**, *69*, 1940.

(67) Sawicka, D.; Houk, K. N. *J. Mol. Model.* **2000**, *6*, 158–165.

(68) Sawicka, D.; Li, Y.; Houk, K. N. *J. Chem. Soc., Perkin Trans. 2* **1999**, 2349–2355.

exothermicity of 65.8 kcal/mol observed for this reaction. The NICS criterion is found to be quite useful in assessing the aromaticity factor in these reactions. Both energetics and the NICS-based aromaticity evaluation clearly supported the **4** to **5**, **6** to **7**, and **14** to **15** conversions as aromaticity-driven processes. Even the nonaromatic intermediate and transition states are not too unstable to stop the reaction. The involvement of a third MeCN molecule was found to be very crucial for the completion of the reaction because it stabilizes the nitride complex by forming an aromatic TiNCN titanacycle. Otherwise, the reaction might have stopped at **9**. The four-membered titanacycles $\overline{TiCHCHCH}$ in **5** and $\overline{TiNC(CH_3)N}$ in **15** are structurally and electronically very interesting because of the 4π electron aromatic character. The stability of these metallacycles comes from the participation of a vacant Ti “d” orbital in the 4π electron conjugation, which is an important factor of aromaticity in metalloaromatic systems as well as the agostic bonding interactions. The reactions described in this work also

support that the phenomenon of aromaticity commonly observed in organic chemistry can be cleverly utilized as an important catalytic element for designing systems capable of breaking strong double and triple bonds. For instance, stable derivatives of **6**, **7**, **9**, or **15** could be considered for developing metathesis catalysts for triple-bonded systems.

Acknowledgment. Support from the following sources are gratefully acknowledged: (i) Grant-in-Aid for the 21st Century COE “Frontiers in Computational Science”; (ii) Research Center for Computational Science, Okazaki, Japan; and (iii) Council of Scientific and Industrial Research (CSIR), India.

Supporting Information Available: Optimized geometries of all the systems and their energy values. This material is available free of charge via the Internet at <http://pubs.acs.org>.

OM060097J